

Enhanced Feature Based Granular Ball Twin Support Vector Machine

A. Quadir¹, M. Sajid¹, Mushir Akhtar¹, M. Tanveer^{1*}, and P. N. Suganthan²

¹ Indian Institute of Technology Indore, Simrol, Indore, India
{mcsphd2207141002, phd2101241003, mtanveer}@iiti.ac.in

² KINDI Center for Computing Research, College of Engineering, Qatar University,
Doha, Qatar
{p.n.suganthan}@qu.edu.qa

Abstract. In this paper, we propose enhanced feature based granular ball twin support vector machine (EF-GBTSVM). EF-GBTSVM employs the coarse granularity of granular balls (GBs) as input rather than individual data samples. The GBs are mapped to the feature space of the hidden layer using random projection followed by the utilization of a non-linear activation function. The concatenation of original and hidden features derived from the centers of GBs gives rise to an enhanced feature space, commonly referred to as the random vector functional link (RVFL) space. This space encapsulates nuanced feature information to GBs. Further, we employ twin support vector machine (TSVM) in the RVFL space for classification. TSVM generates the two non-parallel hyperplanes in the enhanced feature space, which improves the generalization performance of the proposed EF-GBTSVM model. Moreover, the coarser granularity of the GBs enables the proposed EF-GBTSVM model to exhibit robustness to resampling, showcasing reduced susceptibility to the impact of noise and outliers. We undertake a thorough evaluation of the proposed EF-GBTSVM model on benchmark UCI and KEEL datasets. This evaluation encompasses scenarios with and without the inclusion of label noise. Moreover, experiments using NDC datasets further emphasize the proposed model's ability to handle large datasets. Experimental results, supported by thorough statistical analyses, demonstrate that the proposed EF-GBTSVM model significantly outperforms the baseline models in terms of generalization capabilities, scalability, and robustness. The source code for the proposed EF-GBTSVM model, along with additional results and further details, can be accessed at <https://github.com/mtanveer1/EF-GBTSVM>.

Keywords: Random vector functional link network · Extreme learning machine · Twin support vector machine · Granular ball computing · Scalability · Robustness.

* Corresponding Author

1 Introduction

Support vector machine (SVM) [4] stands out as one of the most extensively employed machine learning (ML) models for classification problems. The main objective of SVM is to find the optimal hyperplane, effectively segregating the classes while simultaneously maximizing the margin between the two classes. SVM has found its applications in various real-world problems such as face recognition [7], cancer detection [1], brain-computer interface [20], diagnosis of Schizophrenia disease [38], significant memory concern diagnosis [34] and so on.

SVM addresses a single large quadratic programming problem (QPP), which increases computational complexity and makes it less effective for handling large-scale datasets. To address the computational complexity of SVM, Jayadeva et al. [15] introduced twin SVM (TSVM). TSVM solves two smaller-sized QPPs instead of a single large QPP, making TSVM four times faster compared to SVM [15, 37]. This firmly establishes TSVM as a standout and superior choice due to its efficiency. However, TSVM still requires the computation of matrix inverses and relies on the existence of nonsingular matrices making it not suitable for large scale problems. Numerous adaptations of the TSVM have been suggested to tackle various challenges encountered in classification problems [2, 26, 27]. Notably, among these challenges, the presence of noise stands out as a significant issue. To mitigate the impact of noise, diverse techniques are employed to assign fuzzy membership weights to noisy data points across various applications [30, 28]. Granular ball SVM (GBSVM) [42] and granular ball TSVM with pinball loss (Pin-GBT SVM) [25] are proposed to mitigate the impact of noise and outliers, by incorporating the granular ball (GB) concept into SVM and TSVM. GBSVM and Pin-GBT SVM process inputs in the form of GBs obtained from the dataset instead of considering individual data points. GBSVM and Pin-GBT SVM have showcased proficiency in handling noise and outliers, demonstrating a higher level of accuracy when compared to the standard SVM.

Artificial neural networks (ANNs) are ML models that mimic the structure and functionality of the human brain's neural system. Within ANNs, nodes, also referred to as "neurons," are interconnected in layers. These layers collaborate to process, analyze, and relay information, ultimately enabling the network to make predictions or decisions. ANN has showcased achievements across diverse fields, including stock market prognostication [5], rainfall forecasting [18], clinical medicine [3], solving partial and ordinary differential equations [16, 17], diagnosis of Alzheimer's disease [31], feature interpretability [32] and so on. In addition to numerous advantages, there are certain drawbacks associated with ANN models, such as slow convergence, local minima problems, and sensitivity to learning rates.

To address these challenges, randomized neural networks (RNNs) based on closed-form solutions [36] have been proposed. Generally, a certain level of randomness is inherent in either the structure or the learning process of the RNN model. The presence of randomness in RNN provides them with the capability to learn with fewer tunable parameters in a shorter duration, often eliminating the need for advanced hardware. The random vector functional link (RVFL) neural

network [23, 19] is a widely recognized variant of RNNs. In the RVFL framework, the weights linking the input layer to the hidden layer are randomly generated from a pertinent domain and remain constant throughout the training phase. The direct connections within the RVFL play a pivotal role in determining its generalization performance [43, 40]. The output parameters, encompassing the weights of direct links and the connections linking the hidden layer to the output layer, are analytically computed using techniques such as the least squares method or the pseudo-inverse. Furthermore, the RVFL’s thinner topology, when contrasted with the other popular RNNs such as extreme learning machine or RVFL without direct link (RVFLwoDL) [13], contributes to reduced complexity, aligning with the probably approximately correct (PAC) learning theory and Occam’s principle [35]. The RVFL provides rapid training speed while also possessing universal approximation capabilities [14, 22]. The RVFL demonstrates promising results across various applications, such as data streams [24], electricity load demand forecasting [29], Alzheimer’s disease diagnosis [10, 39], and so on.

Input data samples offer a wide range of information derived from various feature representations. This includes compressed feature representations obtained from lower-dimensional feature spaces as well as sparse feature representations derived from higher-dimensional feature spaces [12, 11]. Different learning algorithms explore various underlying information present in the data through these distinct feature representations. RVFL utilizes random feature transformation in conjunction with the original features and has been effectively employed in tasks related to both classification and regression. Inspired by the achievements associated with diverse feature representations, we propose an enhanced feature-based granular ball twin support vector machine (EF-GBT SVM). EF-GBT SVM model first generates the GBs from the input training data. The centers of generated GBs are then projected to the hidden layer and weights and biases are generated randomly. The hidden layer, endowed with an activation function, serves to convert the input feature space into a randomized feature space. TSVM model is used to train for classification over the enhanced feature space, which is a combination of original features and hidden features of GB centers. The proposed EF-GBT SVM utilizes GBs as input for classifier construction, ensuring heightened robustness, resilience to resampling, and computational efficiency. The proposed EF-GBT SVM model exhibits several notable characteristics:

1. EF-GBT SVM utilizes GBs as inputs and constructs the classifier in the RVFL space, providing enhanced robustness, resilience to resampling, and computational efficiency.
2. Leveraging the principles of granularity, the proposed EF-GBT SVM model effectively addresses the negative impacts of noise and outliers.
3. Training the proposed EF-GBT SVM model in the enhanced feature space elevates its performance by effectively capturing intricate data patterns and complex relationships.
4. The proposed EF-GBT SVM model achieves scalability by using a coarser granularity, allowing it to efficiently manage large datasets.

The rest of the paper is organized as follows: Section 2 gives the information of the related work. We discuss the proposed model in Section 3. Section 4 demonstrates the experimental results. Finally, in Section 5 we conclude by suggesting potential directions for future research.

2 Related Work

This section provides a concise overview of granular ball computing and TSVM.

2.1 Notations

Let $\mathcal{X} = \{(x_i, y_i), i = 1, 2, 3, \dots, n\}$ denotes the training dataset, where $y_i \in \{+1, -1\}$ represents the label of $x_i \in \mathbb{R}^{1 \times m}$. The collection of generated granular balls is represented as $G = \{GB_i, i = 1, 2, \dots, k\} = \{(c_i, t_i), i = 1, 2, \dots, k\}$, where c_i signifies the center, and t_i is the label of the i^{th} granular ball. Let $X = (x_1^t, x_2^t, \dots, x_n^t)^t$ represent the collection of all input samples, where $(\cdot)^t$ represent the transpose operator.

2.2 Granular Ball Computing [41]

In 1996, Lin and Zadeh proposed the idea of “granular computing” aiming to reduce the number of required training data points. The fundamental concept of granular ball computing involves using a hyper ball to enclose either the entire sample space or a specific portion of it. Using the “granular ball” to represent the sample space helps capture multi-granularity learning attributes and allows for a more precise characterization of the sample space. The center “ c ” of a GB is defined as the centroid calculated from all sample points within the ball. Mathematically, it can be expressed as: $c = \frac{1}{l} \sum_{i=1}^l x_i$, where x_i signifies an individual data point and l represents the total number of data points contained within the granular ball. The label assigned to the granular ball is selected by identifying the label that occurs most frequently among the samples contained within the granular ball. To measure the degree of division within a granular ball, the concept of “threshold purity” is introduced. This threshold refers to the proportion of samples within a granular ball that possesses identical labels, particularly the predominant labels.

Let $\mathcal{X} = \{(x_i, y_i), i = 1, 2, 3, \dots, n\}$ be the training dataset. The generated granular ball from the dataset \mathcal{X} is represented as GB_j ($j = 1, 2, 3, \dots, k$). Here k denotes the total number of granular balls generated from the dataset \mathcal{X} . Formally, the solution for generating granular balls is defined by the following optimization problem:

$$\begin{aligned} \min \quad & \vartheta_1 \times \frac{n}{\sum_{i=1}^k |GB_i|} + \vartheta_2 \times k \\ \text{s.t.} \quad & \text{quality}(GB_j) \geq \varphi, \quad j = 1, 2, \dots, k, \end{aligned} \quad (1)$$

where φ denotes the purity threshold, while ϑ_1 and ϑ_2 denote the weight coefficients.

2.3 Twin Support Vector Machine (TSVM) [15]

The main idea of twin support vector machine (TSVM) [15] is to generate two non-parallel hyperplanes, with each plane passing through the corresponding samples of the respective classes and maximizing the distance of the hyperplanes from samples of the other classes. Let $A \in \mathbb{R}^{n_1 \times m}$ and $B \in \mathbb{R}^{n_2 \times m}$ are the input matrices, where n_1 (n_2) is the number of data samples belonging to +1 (-1) class and m is the total number of attributes of each data sample. The formulation of TSVM is given as follows:

$$\begin{aligned} \min_{w_1, b_1} \quad & \frac{1}{2} \|Aw_1 + e_1 b_1\|^2 + d_1 e_2^t \xi_2 \\ \text{s.t.} \quad & -(Bw_1 + e_2 b_1) + \xi_2 \geq e_2, \\ & \xi_2 \geq 0, \end{aligned} \tag{2}$$

and

$$\begin{aligned} \min_{w_2, b_2} \quad & \frac{1}{2} \|Bw_2 + e_2 b_2\|^2 + d_2 e_1^t \xi_1 \\ \text{s.t.} \quad & (Aw_2 + e_1 b_2) + \xi_1 \geq e_1, \\ & \xi_1 \geq 0, \end{aligned} \tag{3}$$

here ξ_1 and ξ_2 denotes the slack vectors, d_1 and d_2 represent the pre-specified penalty parameters and e_1 and e_2 are vectors composed of ones with approximate dimensions.

3 Proposed Enhanced Feature Based Granular Ball Twin Support Vector Machine

In this section, we propose enhanced feature-based granular ball twin support vector machine (EF-GBT SVM). EF-GBT SVM model utilizes granular balls (GBs) as inputs and constructs the classifier within the RVFL space, offering enhanced robustness, resilience to resampling, and computational efficiency. By leveraging the principles of granularity, the proposed EF-GBT SVM model effectively mitigates the negative impacts of noise and outliers, thus addressing the underlying problem of classification in the presence of noisy data. The proposed model can be explained through a three-step process: the initial step involves generating the GB from the input training data. The second step involves feature mapping, where the features of the center of GBs are transformed into an enhanced feature representation (see eqns. 4 and 5). The third step is to construct a classifier using TSVM over the enhanced feature space. TSVM determines the non-parallel decision hyperplanes by utilizing the enhanced features of centers of GBs rather than the original data points.

Let $C \in \mathbb{R}^{k \times m}$ be the centers of the generated GBs of the training dataset \mathcal{X} . The matrix C of the GB is processed through the hidden layers to extract the more important features. Consider a hidden layer with h nodes, $W \in \mathbb{R}^{m \times h}$

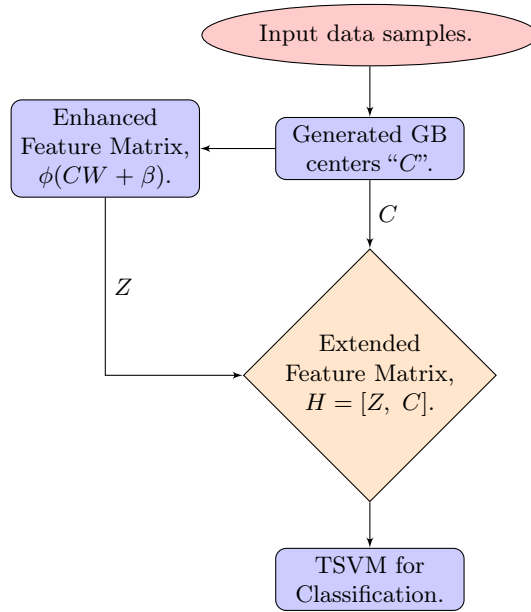


Fig. 1: Flowchart of the proposed EF-GBTSVM model. The entire dataset can be considered as a granular ball (GB). First, calculate the center “ C ” and the label of the GBs. Then, compute the hidden layer matrix “ Z ” for the generated GB center, with weights and biases randomly initialized. Next, obtain the enhanced features (RVFL features) by concatenating the hidden feature “ Z ” with the center matrix “ C ”. Finally, use TSVM to classify the data points into $+1$ and -1 classes, respectively.

represents the weight matrix from the input layer (of centers) to the hidden layer, and β denotes the bias term. The hidden layer matrix Z is defined as:

$$Z = \phi(CW + \beta) \in \mathbb{R}^{k \times h}, \quad (4)$$

where ϕ is the activation function. The enhanced features (RVFL features) are obtained by concatenating the hidden feature Z and the center of generated GB C of training dataset and is defined as:

$$H = [Z, C] \in \mathbb{R}^{k \times (m+h)}. \quad (5)$$

Now, we train our proposed model on enhanced feature space rather than the original feature space. This novel training approach enables the proposed model to capture nuanced features that traditional models like TSVM often overlook. Fig. 1 depicts the flowchart of the proposed EF-GBTSVM model and illustrates the process of transforming the entire dataset into a GB. It shows the calculation of the center “ C ” and the hidden layer matrix “ Z ”. The enhanced features are obtained by concatenating the hidden feature “ Z ” with the center matrix “ C ”, followed by the TSVM classification into $+1$ and -1 classes.

Let $H = T_1 \cup T_2$, where $T_1 = [Z^+, C^+] \in \mathbb{R}^{k_1 \times (m+h)}$ and $T_2 = [Z^-, C^-] \in \mathbb{R}^{k_2 \times (m+h)}$ represent the enhanced feature matrices of +1 and -1 class. Here, Z^+ and Z^- represent the hidden layer matrix +1 and -1 class and C^+ and C^- represent the generated GB center matrix of +1 and -1 class, and k_1 and k_2 are the number of GBs of +1 and -1 class, respectively. The objective function of the proposed EF-GBT SVM model is formally defined as follows:

$$\begin{aligned} \min_{w_1, b_1} \quad & \frac{1}{2} \|T_1 w_1 + e_1 b_1\|^2 + d_1 e_2^t \xi_2 \\ \text{s.t.} \quad & -(T_2 w_1 + e_2 b_1) + \xi_2 \geq e_2, \\ & \xi_2 \geq 0, \end{aligned} \quad (6)$$

and

$$\begin{aligned} \min_{w_2, b_2} \quad & \frac{1}{2} \|T_2 w_2 + e_2 b_2\|^2 + d_2 e_1^t \xi_1 \\ \text{s.t.} \quad & T_1 w_2 + e_1 b_2 + \xi_1 \geq e_1, \\ & \xi_1 \geq 0, \end{aligned} \quad (7)$$

where $w_1 \in \mathbb{R}^{(m+h) \times 1}$, $b_1 \in \mathbb{R}$, $w_2 \in \mathbb{R}^{(m+h) \times 1}$, $b_2 \in \mathbb{R}$, $\xi_2 \in \mathbb{R}^{k_2 \times 1}$, and $\xi_1 \in \mathbb{R}^{k_1 \times 1}$. d_1 and d_2 are the tunable parameters. e_1 and e_2 are the vectors of ones of appropriate dimensions.

The Lagrangian corresponding to the problem (6) is given by

$$L = \frac{1}{2} \|T_1 w_1 + e_1 b_1\|^2 + d_1 e_2^t \xi_2 - \alpha^t (-(T_2 w_1 + e_2 b_1) + \xi_2 - e_2) - \beta^t \xi_2, \quad (8)$$

where $\beta \in \mathbb{R}^{k_2 \times 1}$ and $\alpha \in \mathbb{R}^{k_2 \times 1}$ are the vectors of Lagrangian multipliers. The optimal conditions are given as follows:

$$T_1^t (T_1 w_1 + e_1 b_1) + T_2^t \alpha = 0, \quad (9)$$

$$e_1^t (T_1 w_1 + e_1 b_1) + e_2^t \alpha = 0, \quad (10)$$

$$e_2 d_1 - \alpha - \beta = 0, \quad (11)$$

$$-(T_2 w_1 + e_2 b_1) + \xi_2 \geq e_2, \quad \xi_2 \geq 0, \quad (12)$$

$$\alpha^t (-(T_2 w_1 + e_2 b_1) + \xi_2 - e_2) = 0, \quad \beta^t \xi_2 = 0, \quad (13)$$

$$\alpha \geq 0, \quad \beta \geq 0. \quad (14)$$

Combining (9) and (10) leads to

$$\begin{pmatrix} T_1^t \\ e_1^t \end{pmatrix} (T_1 \ e_1) \begin{pmatrix} w_1 \\ b_1 \end{pmatrix} + \begin{pmatrix} T_2^t \\ e_2^t \end{pmatrix} \alpha = 0. \quad (15)$$

Let $H = (T_1 \ e_1)$, $G = (T_2 \ e_2)$ and $u_1 = \begin{pmatrix} w_1 \\ b_1 \end{pmatrix}$ then, (15) can be reformulated as:

$$\begin{aligned} H^t H u + G^t \alpha &= 0, \\ \text{i.e., } u_1 &= -(H^t H)^{-1} G^t \alpha. \end{aligned} \quad (16)$$

Computing the inverse of H^tH presents a formidable challenge. However, this difficulty can be effectively addressed by incorporating a regularization term denoted as δI in (16), where I represents an identity matrix of suitable dimensions. Thus,

$$u_1 = -(H^tH + \delta I)^{-1}G^t\alpha. \quad (17)$$

Using eqn. (17) and the above K.K.T. conditions, we can obtain the dual of (6) as follows:

$$\begin{aligned} \max_{\alpha} \quad & \alpha^t e_2 - \frac{1}{2}\alpha^t E(F^tF + \delta I)^{-1}E^t\alpha \\ \text{s.t.} \quad & 0 \leq \alpha \leq d_1 e_2, \end{aligned} \quad (18)$$

Likewise, the Wolfe dual for (7) can be obtained as

$$\begin{aligned} \max_{\gamma} \quad & \gamma^t e_1 - \frac{1}{2}\gamma^t F(E^tE + \delta I)^{-1}F^t\gamma \\ \text{s.t.} \quad & 0 \leq \gamma \leq d_2 e_1, \end{aligned} \quad (19)$$

where $F = (T_1 \ e_1)$, $E = (T_2 \ e_2)$ and $u_1 = \begin{pmatrix} w_1 \\ b_1 \end{pmatrix}$, $u_2 = \begin{pmatrix} w_2 \\ b_2 \end{pmatrix}$ is calculated as:

$$u_1 = -(F^tF + \delta I)^{-1}E^t\alpha \text{ and } u_2 = (E^tE + \delta I)^{-1}F^t\gamma. \quad (20)$$

Analogously, $u_2 = \begin{pmatrix} w_2 \\ b_2 \end{pmatrix}$ corresponding to the -1 class can be calculated by the subsequent eqn.:

$$u_2 = (G^tG + \delta I)^{-1}H^t\gamma. \quad (21)$$

Once the optimal u_1 and u_2 are obtained, the following decision function can be used to predict the target value of a new sample:

$$\text{class}(x) = \arg \min_{i \in \{1,2\}} \frac{|w_i^t x + b_i|}{\|w_i\|}. \quad (22)$$

The time complexity and algorithm of the proposed EF-GBTSVM model are discussed in Section S.I. of the file available on our GitHub repository. Also, we give the theoretical comparison of the proposed EF-GBTSVM model w.r.t. the baseline GBSVM and TSVM models in Section S.II is provided in Section S.II of the same file.

4 Experimental Results

To evaluate the effectiveness of the proposed EF-GBTSVM model, we conduct a comparative analysis along with the baseline models on benchmark datasets from the UCI [9] and KEEL [8] repository. Moreover, we performed experiments using datasets generated through the NDC Data Generator [21].

4.1 Experimental Setup

The experimental setup includes a PC with an Intel(R) Xeon(R) Gold 6226R CPU operating at 2.90 GHz and 128 GB of RAM. This system operates on the Windows 11 platform and utilizes Python 3.11 for execution. The dual QPP arising in the proposed EF-GBT SVM model and the baseline models are solved by the “qp-solvers” function available in the CVXOPT package. The dataset is randomly partitioned into training and testing subsets at a ratio of 70 : 30, respectively. We use a 5-fold cross-validation method combined with a grid search approach to fine-tune the models’ hyperparameters within designated ranges, $d_1 = d_2 = \{10^{-5}, 10^{-4}, \dots, 10^5\}$. The number of hidden nodes is chosen from the range 3 to 203 with a step size of 20. We tuned nine different activation functions. The indexing of these functions is as follows: 1) SELU, 2) ReLU, 3) Sigmoid, 4) Sine, 5) Hardlim, 6) Tribas, 7) Radbas, 8) Sign, and 9) Leaky ReLU.

4.2 Experiments on Benchmark UCI and KEEL Datasets

In this subsection, we analyze and compare the proposed EF-GBT SVM model along with the baseline SVM [4], GBSVM [42], TSVM [15], RVFLwoDL [13], and RVFL [23] models on 29 UCI and KEEL benchmark datasets. Additionally, we apply the TSVM model on the hidden feature space of the GB centers to assess the significance of enhanced features compared to individually considering the hidden and original features - the resultant model is named hidden feature based granular ball TSVM (HF-GBT SVM).

The experimental outcomes depicted in Table 1 represent the performance of the proposed models along with the baseline models. The accuracy-based comparison reveals that our proposed EF-GBT SVM demonstrates superior performance compared to the baseline SVM, GBSVM, TSVM, RVFLwoDL, and RVFL models across the majority of datasets. From Table 1, the average accuracy (ACC) for our proposed EF-GBT SVM model stands at 86.66%. In contrast, the average ACC of the SVM, GBSVM, TSVM, RVFLwoDL, RVFL and HF-GBT SVM models are 81.18%, 72.22%, 63.78%, 84.04%, 84.55%, and 82.63%, respectively. The average ACC metric can be influenced by outstanding performance in a single dataset, which could compensate for weaker results across various datasets, potentially resulting in a biased measure. Therefore, we apply a ranking method to assess the effectiveness and evaluate the performance of the models. In this approach, classifiers are ranked based on their performance: models with better performance receive a lower rank, while those with poorer performance are given a higher rank. To evaluate q models across P datasets, r_j^i denotes the rank of the j^{th} model on the i^{th} dataset. $\mathcal{R}_j = \frac{1}{P} \sum_{i=1}^P r_j^i$ is the average rank of the model. The average rank of proposed EF-GBT SVM models along with the HF-GBT SVM, SVM, GBSVM, TSVM, RVFLwoDL, and RVFL models are 2.14, 3.81, 3.9, 5.26, 6.66, 3.03, and 3.21, respectively. The proposed EF-GBT SVM exhibits the most favorable average rank among the compared models. Therefore, the proposed EF-GBT SVM model demonstrates

superior generalization ability compared to the baseline models. A notable finding is that the proposed EF-GBTSVM (on enhanced feature space) outperforms HF-GBTSVM (on hidden feature space) and TSVM (on original feature space). This shows the clear significance of training the classifier over the enhanced feature space over the individual original and hidden feature spaces.

Datasets	SVM [4]	GBSVM [42]	TSVM [15]	RVFLwoDL [13]	RVFL [23]	HF-GBTSVM [†]	EF-GBTSVM [†]
aus	88.46	81.11	64.31	87.98	86.94	85.1	88.96
breast_cancer	72.09	62.79	60	74.42	72.09	73.26	78.14
checkerboard_Data	85.46	71.06	64.31	85.98	85.94	85.1	86.21
chess_krvkp	84.67	69.62	67.41	90.2	90.41	90.09	98.16
crossplane130	97.24	100	71.35	97.44	97.44	100	100
ecoli-0-1-4-7_vs_5-6	87	76	67.32	90	90	94	94
ecoli-0-1-4-6_vs_5	95.81	94.05	67.88	98.81	98.81	89.29	97.62
ecoli-0-1_vs_2-3-5	81.89	77.3	68.24	80.59	80.59	90.54	82.43
haber	77.17	77.17	57.96	76.09	78.26	76.09	79.35
haberman	77.17	77.17	57.96	76.09	76.09	70.65	76.09
haberman_survival	77.17	78.26	57.96	78.26	76.09	73.91	78.13
heart-stat	90.12	85.93	58.69	81.89	81.89	81.48	86.42
led7digit-0-2-4-5-6-7-8-9_vs_1	92.23	78.35	66.77	94.74	94.74	84.96	94.74
mammographic	79.58	80.28	60.41	82.35	82.01	75.43	83.74
monks_3	75.45	59.88	59.7	43.11	43.11	88.62	92.22
musk_1	68.53	52.66	59.15	81.44	84.62	79.02	79.72
new-thyroid1	88.46	85.38	66	86	86	81.54	86.15
ooocytes_merluccius_nucleus_4d	64.82	63.19	59.58	82.74	80.71	75.9	81.13
spectf	76.54	70.4	62.39	85.19	83.95	81.48	81.48
tic_tac_toe	75.69	76.88	68.66	96.65	96.65	99.65	99.65
vehicle1	76.38	73.62	59.44	81.86	81.68	83.46	81.89
vehicle2	71.65	53.54	64.86	90.03	90.85	93.31	92.52
vertebral_column_2classes	75.27	68.82	63.13	82.25	81.4	88.17	72.04
wpbc	77.97	57.63	60	70.97	69.49	77.97	71.19
yeast-0-5-6-7-9_vs_4	81.19	56.6	68.29	76.1	93.71	76.1	94.34
yeast-0-2-5-7-9_vs_3-6-8	86.79	68.55	66.67	95.68	95.35	64.24	95.03
yeast-0-2-5-6_vs_3-7-8-9	83.71	64.9	66.23	89.71	89.71	62.91	90.07
yeast3	79.91	79.03	67.15	85.07	86.72	86.77	89.46
yeast-2_vs_4	85.81	54.19	67.7	95.48	96.77	87.1	83.23
Average ACC	81.18	72.22	63.78	84.04	84.55	82.63	86.66

[†] represents the proposed models. Bold text denotes the model with the highest average ACC.

Table 1: Comparison results on benchmark UCI and KEEL datasets for the proposed EF-GBTSVM model with the baseline models.

We now conduct statistical tests to determine the significance of the results. Specifically, we use the Friedman test [6] to evaluate whether there are statistically significant differences between the models. Under the null hypothesis, it is assumed that all models have the same average rank, suggesting that they perform at the same level. The Friedman statistic, which follow the chi-squared distribution (χ_F^2) with $(q - 1)$ degrees of freedom (d.o.f), and its computation involves: $\chi_F^2 = \frac{12P}{q(q+1)} \left[\sum_j \mathcal{R}_j^2 - \frac{q(q+1)^2}{4} \right]$. The F_F statistic is computed as $F_F = \frac{(P-1)\chi_F^2}{P(q-1)-\chi_F^2}$, where the F -distribution possesses degrees of freedom $(q - 1)$ and $(P - 1) \times (q - 1)$. For $q = 7$ and $P = 29$, the obtained values are $\chi_F^2 = 85.8435$ and $F_F = 27.2654$. The critical value $F_F(6, 168) = 2.1529$ at a 5% level of significance. We reject the null hypothesis as $27.2654 > 2.1529$. Thus, there exists a statistically significant difference among the models being compared. Next, we employ the Nemenyi post hoc test to examine the pairwise differences between the models. The critical difference ($C.D.$) value is calculated as $C.D. = q_\alpha \sqrt{\frac{q(q+1)}{6P}}$. The critical value $q_\alpha = 2.949$ is employed to

Datasets	Noise	SVM [4]	GBSVM [42]	TSVM [15]	RVFLwoDL [13]	RVFL [23]	HF-GBTSVM [†]	EF-GBTSVM [†]
chess_krvkp	5%	84.25	84.78	83.85	90.68	90.68	87.07	93.22
	10%	84.36	77.75	85.1	91.89	92.64	87.07	90.82
	15%	85.61	82.83	84.37	89.74	90.12	89.68	90.41
	20%	86.55	64.55	82.81	90.2	89.7	80.4	88.11
led7digit-0-2-4-5-6-7-8-9_vs_1	5%	83.23	78.35	83.98	80.17	81.1	83.61	84.6
	10%	83.23	90.98	84.74	94.74	94.74	83.61	94.98
	15%	83.23	68.42	84.74	93.98	92.48	95.97	83.46
	20%	93.23	80.41	83.74	83.98	83.98	87.97	84.44
monks_3	5%	73.65	59.88	77.25	95.21	95.21	92.81	92.81
	10%	73.05	70.66	76.65	94.01	94.01	92.81	94.42
	15%	73.05	70.06	70.44	91.62	92.22	94.42	95.03
	20%	71.86	80	71.26	89.22	89.82	82.04	90.84
tic_tac_toe	5%	75.35	70.47	95.65	97.65	97.65	98.28	99.65
	10%	76.04	70.97	89.65	92.31	92.31	98.28	99.65
	15%	74.65	60.76	89.65	97.65	98.31	97.65	98.61
	20%	73.96	63.33	89.65	92.92	97.92	93.75	98.96
vehicle1	5%	76.27	69.82	88.17	80.17	82.6	78.42	91.4
	10%	75.27	68.82	89.25	81.25	85.25	77.42	81.27
	15%	74.19	68.82	79.25	82.17	82.17	83.87	83.12
	20%	69.82	68.48	76.02	88.17	89.57	75.64	82.04
yeast3	5%	80.81	81.26	81.48	91.17	91.27	91.48	94.55
	10%	89.69	82.74	89.69	93.95	90.5	91.48	90.77
	50%	89.46	82.87	88.79	90.83	90.72	80.7	89.46
	20%	88.12	76.23	80.81	90.38	93.05	89.01	93.24
Average ACC	5%	78.93	74.09	85.06	89.18	89.75	88.61	92.71
	10%	80.27	76.99	85.85	91.36	91.58	88.45	91.99
	15%	80.03	72.29	82.87	91	91	90.38	90.02
	20%	80.59	72.17	80.72	89.15	90.84	84.8	89.61

[†] represents the proposed models. Bold text denotes the model with the highest average ACC.

Table 2: Classification accuracy (ACC) over UCI and KEEL datasets with different percentages of label noise.

evaluate 7 models at a significance level of 5%. After simple calculation, we obtain $C.D. = 1.672$. The difference in average ranks between pairs of models EF-GBTSVM with SVM, GBSVM, TSVM, RVFLwoDL, RVFL, and HF-GBTSVM are 1.76, 3.12, 4.52, 0.89, 1.07, and 1.67. The proposed EF-GBTSVM model exhibits significant differences from the baseline models, except RVFL, RVFLwoDL, and HF-GBTSVM. However, the average rank of the proposed EF-GBTSVM model surpasses the RVFL, RVFLwoDL, and HF-GBTSVM models. Hence, the proposed EF-GBTSVM model showcases superior performance against the baseline models and HF-GBTSVM. We discuss the sensitivity analysis and ablation study of the proposed EF-GBTSVM model in Sections S.III and S.IV of the file available on our GitHub repository.

4.3 Evaluation on UCI and KEEL Datasets with Label Noise

While the UCI datasets employed in our study are representative of real-world scenarios, it is crucial to acknowledge that the presence of impurities or noise in collected data can escalate due to various factors. In such circumstances, the development of a robust model becomes imperative, capable of effectively addressing and handling these challenging scenarios. To showcase the superiority of the proposed EF-GBTSVM model even in adverse conditions, the label noise is introduced at varying levels of 5%, 10%, 15%, and 20%. We have selected 6 diverse UCI and KEEL datasets for our comparative analysis. The result presented in Table 2 demonstrates the effectiveness of these models compared to the baseline SVM, GBSVM, TSVM, RVFLwoDL, RVFL, and HF-GBTSVM models. From the Table 2, the proposed EF-GBTSVM model exhibited a top

NDC datasets	SVM [4]	GBSVM [42]	T SVM [15]	RVFLwoDL [13]	RVFL [23]	HF-GBTSVM [†]	EF-GBTSVM [†]
	ACC (%) Time (s)	ACC (%) Time (s)	ACC (%) Time (s)	ACC (%) Time (s)	ACC (%) Time (s)	ACC (%) Time (s)	ACC (%) Time (s)
Train 10k	80.64	52.43	86.59	73.17	75.77	78.79	78.79
	309.03	1044.219	209.606	0.937	0.937	0.344	0.275
Train 50k	79.42	53.41	86.21	80.11	80.94	79.6	81.6
	809.5467	2478.142	715.689	0.453	0.453	0.498	0.462
Train 1l	a	b	a	78.63	78.3	78.87	83.01
Train 3l	a	b	a	0.944	0.944	0.86	0.844
				79.52	80.97	80.1	81.33
Train 5l	a	b	a	2.702	2.702	2.127	2.015
				81.15	82.38	81.67	83.97
Train 1m	a	b	a	11.454	11.454	2.924	2.33
				81.57	81.66	81.95	82.45
Train 3m	a	b	a	69.031	69.031	6.244	6.25
				80.44	80.87	82.04	82.22
Train 5m	a	b	a	76.725	76.725	19.054	16.744
				83.61	84.04	84.18	83.71
Train 1cr	a	b	a	83.1	83.93	35.982	30.312
				82.79	82.88	84.66	85.21
				92.64	91.44	62.33	57.212

^a Terminated because of out of memory.

^b Experiment is terminated because of the out of bound issue shown by PSO algorithm.

[†] represents the proposed models. Bold text denotes the model with the highest average ACC.

Table 3: Comparison results on benchmark NDC datasets for the proposed EF-GBTSVM model with the baseline models.

position compared to the existing models. The average ACC of the proposed EF-GBTSVM model at 5%, 10%, 15%, and 20% level of noise are 92.71%, 91.99%, 90.02% and 89.61%, respectively. The average ACC of the EF-GBTSVM model is highest at 5%, 10%, 15%, and 20% level of noise except RVFL, RVFLwoDL, and HF-GBTSVM at 15% level of noise. This significant difference in accuracies highlights the superior performance and effectiveness of the proposed EF-GBTSVM model relative to the existing baseline models. The observations mentioned above emphasize the importance of the proposed EF-GBTSVM model as a robust model with improved feature extraction capabilities. The proposed model showcases an adept ability to navigate and excel in scenarios where noise and impurities pose substantial challenges.

4.4 Experiment on NDC Datasets

The preceding comprehensive analyses consistently reveal the superior performance of the proposed EF-GBTSVM model in comparison to the baseline models across the majority of UCI and KEEL benchmark datasets. Now, we conduct an experiment utilizing the NDC datasets [21] to emphasize the improved training speed and scalability of our proposed models. For this, the hyperparameters d_1 and d_2 are set to 1 to reduce the training time. The sample sizes of these NDC datasets range from 10k to 1cr, each containing 32 features. The results depicted in Table 3 demonstrate the efficiency and scalability of the proposed EF-GBTSVM model. Across the NDC datasets, our proposed model consistently surpass the baseline models in both ACC and training times, affirming their robustness and efficiency, especially when handling large-scale datasets. In terms of

ACC, our proposed EF-GBTSVM model exhibits superior performance, achieving up to 3% increase in ACC compared to baseline models on large datasets. Furthermore, our proposed model demonstrates reduced training time in comparison to the compared existing models. The experimental findings indicate that the proposed EF-GBTSVM model exhibits efficient training speed, surpassing some baseline models by several hundred or even a thousand times. This reduction in training time can be attributed to the considerably lower count of generated GBs on a dataset compared to the total number of samples.

5 Conclusions

This paper proposed an enhanced feature based granular ball twin support vector machine (EF-GBTSVM). EF-GBTSVM employs the coarse granularity of GBs as input, resulting in the formation of two non-parallel hyperplanes in the enhanced feature space. The proposed EF-GBTSVM reduces the impact of noise and outliers while alleviating the challenge of high computational costs. To demonstrate the effectiveness, robustness, scalability, and efficiency of our proposed EF-GBTSVM model, we conducted a comprehensive series of experiments supported by detailed statistical analyses. These analyses encompass various ranking schemes, including the Friedman and Nemenyi post hoc tests. Furthermore, by adding label noise to the UCI and KEEL datasets, we evaluated the robustness of our proposed model in comparison to baseline models under noisy conditions. We evaluated the performance of our models on NDC datasets, varying sample sizes from $10k$ to $1cr$ samples, with a specific emphasis on scalability. Our proposed models have showcased better efficiency, surpassing various baseline models by a factor of 100 to 1000. Although our proposed models have shown excellent performance in binary classification tasks, their effectiveness in multiclass scenarios has not yet been explored. A key direction for future research will be to adapt these models to effectively address multiclass problems. Additionally, enhancing the model by integrating a robust loss function [33], leveraging the L_1 norm for regularization, and incorporating an intuitionistic fuzzy membership scheme could further bolster their robustness and efficacy.

Bibliography

- [1] M. Akhtar, M. Tanveer, and M. Arshad. RoBoSS: A robust, bounded, sparse, and smooth loss function for supervised learning. *arXiv preprint arXiv:2309.02250*, 2023.
- [2] M. Akhtar, M. Tanveer, M. Arshad, and Alzheimer’s Disease Neuroimaging Initiative and others. Advancing supervised learning with the wave loss function: A robust and smooth approach. *Pattern Recognition*, page 110637, 2024, <https://doi.org/10.1016/j.patcog.2024.110637>.
- [3] W. G. Baxt. Application of artificial neural networks to clinical medicine. *The Lancet*, 346(8983):1135–1138, 1995.
- [4] C. Cortes and V. Vapnik. Support-vector networks. *Machine Learning*, 20: 273–297, 1995.
- [5] R. Dase and D. Pawar. Application of artificial neural network for stock market predictions: A review of literature. *International Journal of Machine Intelligence*, 2(2):14–17, 2010.
- [6] J. Demšar. Statistical comparisons of classifiers over multiple data sets. *The Journal of Machine Learning Research*, 7:1–30, 2006.
- [7] O. Déniz, M. Castrillon, and M. Hernández. Face recognition using independent component analysis and support vector machines. *Pattern Recognition Letters*, 24(13):2153–2157, 2003.
- [8] J. Derrac, S. Garcia, L. Sanchez, and F. Herrera. KEEL data-mining software tool: Data set repository, integration of algorithms and experimental analysis framework. *J. Mult. Valued Log. Soft Comput*, 17:255–287, 2015.
- [9] D. Dua and C. Graff. UCI machine learning repository. *Available: <http://archive.ics.uci.edu/ml>*, 2017.
- [10] M. A. Ganaie, M. Sajid, A. K. Malik, and M. Tanveer. Graph embedded intuitionistic fuzzy random vector functional link neural network for class imbalance learning. *IEEE Transactions on Neural Networks and Learning Systems*, pages 1–10, 2024. <https://doi.org/10.1109/TNNLS.2024.3353531>.
- [11] G. E. Hinton and R. R. Salakhutdinov. Reducing the dimensionality of data with neural networks. *Science*, 313(5786):504–507, 2006.
- [12] G. E. Hinton, S. Osindero, and Y.-W. Teh. A fast learning algorithm for deep belief nets. *Neural Computation*, 18(7):1527–1554, 2006.
- [13] G.-B. Huang, Q.-Y. Zhu, and C.-K. Siew. Extreme learning machine: theory and applications. *Neurocomputing*, 70(1-3):489–501, 2006.
- [14] B. Igel'nik and Y.-H. Pao. Stochastic choice of basis functions in adaptive function approximation and the functional-link net. *IEEE Transactions on Neural Networks*, 6(6):1320–1329, 1995.
- [15] Jayadeva, R. Khemchandani, and S. Chandra. Twin support vector machines for pattern classification. *IEEE Transactions on Pattern Analysis and Machine Intelligence*, 29(5):905–910, 2007.

- [16] I. E. Lagaris, A. Likas, and D. I. Fotiadis. Artificial neural networks for solving ordinary and partial differential equations. *IEEE Transactions on Neural Networks*, 9(5):987–1000, 1998.
- [17] I. E. Lagaris, A. C. Likas, and D. G. Papageorgiou. Neural-network methods for boundary value problems with irregular boundaries. *IEEE Transactions on Neural Networks*, 11(5):1041–1049, 2000.
- [18] K. C. Luk, J. E. Ball, and A. Sharma. An application of artificial neural networks for rainfall forecasting. *Mathematical and Computer Modeling*, 33(6-7):683–693, 2001.
- [19] A. K. Malik, R. Gao, M. A. Ganaie, M. Tanveer, and P. N. Suganthan. Random vector functional link network: recent developments, applications, and future directions. *Applied Soft Computing*, page 110377, 2023, <https://doi.org/10.1016/j.asoc.2023.110377>.
- [20] G. N. G. Molina, T. Ebrahimi, and J.-M. Vesin. Joint time-frequency-space classification of EEG in a brain-computer interface application. *EURASIP Journal on Advances in Signal Processing*, 2003:1–17, 2003.
- [21] D. R. Musicant. NDC: normally distributed clustered datasets, 1998. www.cs.wisc.edu/dmi/svm/ndc/.
- [22] D. Needell, A. A. Nelson, R. Saab, and P. Salanevich. Random vector functional link networks for function approximation on manifolds. *arXiv preprint arXiv:2007.15776*, 2020.
- [23] Y.-H. Pao, G.-H. Park, and D. J. Sobajic. Learning and generalization characteristics of the random vector functional-link net. *Neurocomputing*, 6(2):163–180, 1994.
- [24] M. Pratama, P. P. Angelov, E. Lughofer, and M. J. Er. Parsimonious random vector functional link network for data streams. *Information Sciences*, 430:519–537, 2018.
- [25] A. Quadir and M. Tanveer. Granular ball twin support vector machine with pinball loss function. *IEEE Transactions on Computational Social Systems*, 2024, 10.1109/TCSS.2024.3411395.
- [26] A. Quadir and M. Tanveer. Multiview learning with twin parametric margin SVM. *Neural Networks*, page 106598, 2024, <https://doi.org/10.1016/j.neunet.2024.106598>.
- [27] A. Quadir, M. Akhtar, and M. Tanveer. Enhancing multiview synergy: Robust learning by exploiting the wave loss function with consensus and complementarity principles. *arXiv preprint arXiv:2408.06819*, 2024.
- [28] A. Quadir, M. A. Ganaie, and M. Tanveer. Intuitionistic fuzzy generalized eigenvalue proximal support vector machine. *Neurocomputing*, page 128258, 2024, <https://doi.org/10.1016/j.neucom.2024.128258>.
- [29] Y. Ren, P. N. Suganthan, N. Srikanth, and G. Amaratunga. Random vector functional link network for short-term electricity load demand forecasting. *Information Sciences*, 367:1078–1093, 2016.
- [30] S. Rezvani, X. Wang, and F. Pourpanah. Intuitionistic fuzzy twin support vector machines. *IEEE Transactions on Fuzzy Systems*, 27(11):2140–2151, 2019.

- [31] M. Sajid, A. K. Malik, and M. Tanveer. Intuitionistic fuzzy broad learning system: Enhancing robustness against noise and outliers. *IEEE Transactions on Fuzzy Systems*, 32(8):4460–4469, 2024. <https://doi.org/10.1109/TFUZZ.2024.3400898>.
- [32] M. Sajid, A. K. Malik, M. Tanveer, and P. N. Suganthan. Neuro-fuzzy random vector functional link neural network for classification and regression problems. *IEEE Transactions on Fuzzy Systems*, 32(5):2738–2749, 2024. <https://doi.org/10.1109/TFUZZ.2024.3359652>.
- [33] M. Sajid, A. Quadir, and M. Tanveer. Wave-RVFL: A randomized neural network based on wave loss function. In *Proceedings of the 27th International Conference on Neural Information Processing*, 2024. URL <https://arxiv.org/abs/2408.02824>.
- [34] M. Sajid, R. Sharma, I. Beheshti, M. Tanveer, and for the Alzheimer’s Disease Neuroimaging Initiative. Decoding cognitive health using machine learning: A comprehensive evaluation for diagnosis of significant memory concern. *WIREs Data Mining and Knowledge Discovery*, page e1546, 2024. <https://doi.org/10.1002/widm.1546>.
- [35] Q. Shi, R. Katuwal, P. N. Suganthan, and M. Tanveer. Random vector functional link neural network based ensemble deep learning. *Pattern Recognition*, 117:107978, 2021.
- [36] P. N. Suganthan. On non-iterative learning algorithms with closed-form solution. *Applied Soft Computing*, 70:1078–1082, 2018.
- [37] M. Tanveer, T. Rajani, R. Rastogi, Y.-H. Shao, and M. A. Ganaie. Comprehensive review on twin support vector machines. *Annals of Operations Research*, pages 1–46, 2022, <https://doi.org/10.1007/s10479-022-04575-w>.
- [38] M. Tanveer, M. A. Ganaie, A. Bhattacharjee, and C. T. Lin. Intuitionistic fuzzy weighted least squares twin svms. *IEEE Transactions on Cybernetics*, 53(7):4400–4409, 2023. <https://doi.org/10.1109/TCYB.2022.3165879>.
- [39] M. Tanveer, T. Goel, R. Sharma, A. K. Malik, I. Beheshti, J. Del Ser, P. N. Suganthan, and C. T. Lin. Ensemble deep learning for alzheimer’s disease characterization and estimation. *Nature Mental Health*, pages 1–13, 2024, <https://doi.org/10.1038/s44220-024-00237-x>.
- [40] N. Vuković, M. Petrović, and Z. Miljković. A comprehensive experimental evaluation of orthogonal polynomial expanded random vector functional link neural networks for regression. *Applied Soft Computing*, 70:1083–1096, 2018.
- [41] S. Xia, Y. Liu, X. Ding, G. Wang, H. Yu, and Y. Luo. Granular ball computing classifiers for efficient, scalable and robust learning. *Information Sciences*, 483:136–152, 2019.
- [42] S. Xia, X. Lian, G. Wang, X. Gao, J. Chen, and X. Peng. GBSVM: An efficient and robust support vector machine framework via granular-ball computing. *IEEE Transactions on Neural Networks and Learning Systems*, 2024, 10.1109/TNNLS.2024.3417433.
- [43] L. Zhang and P. N. Suganthan. A comprehensive evaluation of random vector functional link networks. *Information Sciences*, 367:1094–1105, 2016.

Supplementary Material

S.I Time complexity and algorithm of the proposed EF-GBTSVM model

The complexity of the proposed EF-GBTSVM model mainly hinges on three factors: (a) the computation of granular balls, (b) the necessity of matrix multiplication to generate the hidden feature matrix, and (c) the use of TSVM for classification. The time complexity of standard TSVM [15] is $\mathcal{O}(\frac{n^3}{4})$. Our approach begins with the training dataset \mathcal{X} , which we consider as the initial granular ball (GB) set. We initially divide this GB into two granular balls using the 2-means clustering method, with a time complexity of $\mathcal{O}(2n)$. In subsequent phases, if both granular balls are impure, they are further divided into four granular balls, each maintaining a maximum time complexity of $\mathcal{O}(2n)$. This iterative process continues for a total of *iter* iterations. Therefore, the overall time complexity of generating granular balls is $\mathcal{O}(iter \times 2n)$ or less, accounting for the maximum time complexity per iteration and the total number of iterations *iter*. Generating the hidden feature matrix H involves multiplying the generated granular ball center matrix by randomly generated weights, with a time complexity of $\mathcal{O}(k^2h)$. Hence, the overall time complexity of the proposed EF-GBTSVM is (or less than) $\mathcal{O}(\frac{k^3}{4}) + \mathcal{O}(iter \times 2n) + \mathcal{O}(k^2h)$, where k represents the total number of generated granular balls and h represents the number of hidden nodes. The detailed algorithm of the proposed EF-GBTSVM model, as outlined in 1.

S.II Comparison of the proposed EF-GBTSVM model w.r.t. the baseline GBSVM and TSVM models

This section outlines the difference between the proposed EF-GBTSVM model and existing GBSVM and TSVM models.

– EF-GBTSVM vs GBSVM

- The proposed EF-GBTSVM model solves two quadratic programming problems (QPPs) to determine the optimal parameters. However, GBSVM solves one large QPP to obtain the optimal hyperplanes, leading to an increase in time complexity compared to the proposed models.
- The proposed models utilize the external package "CVXOPT" to solve the dual of the QPPs, employing the "qp-solvers" function to obtain the global solution, whereas, GBSVM employs the PSO algorithm (an iterative method), which may converge to local minima rather than the global minimum.

– EF-GBTSVM vs TSVM

- The proposed model's effectiveness is attributed to its utilization of granular balls as inputs rather than individual sample points. This allows the

Algorithm 1 Algorithm of the proposed EF-GBT SVM model.

Input: Purity threshold η , and the training dataset \mathcal{X} .**Output:** Model parameters.

- 1: Assume the entire dataset \mathcal{X} is represented as a granular ball GB and set of granular balls, G , to be empty set, i.e., $GB = T$ and $G = \{ \}$.
 - 2: $Temp = \{GB\}$.
 - 3: *for* $i = 1 : |Temp|$
 - 4: *if* $pur(GB_i) < \eta$
 - 5: Split GB_i into GB_{i1} and GB_{i2} , using 2-means clustering algorithm.
 - 6: $Temp \leftarrow GB_{i1}, GB_{i2}$.
 - 7: *else*
 - 8: Compute the center $c_i = \frac{1}{p} \sum_{j=1}^p x_j$ of GB_i , where $x_j \in GB_i$, $j = 1, 2, \dots, p$, and p is the number of training sample in GB_i .
 - 9: Compute the label t_i of GB_i , where t_i is assigned the label of majority class samples within GB_i .
 - 10: Put $GB_i = \{(c_i, t_i)\}$ in G .
 - 11: *end if*
 - 12: *end for*
 - 13: *if* $Temp \neq \{ \}$
 - 14: Go to step 3 (for further splitting).
 - 15: *end if*
 - 16: Set $G = \{GB_i, i = 1, 2, \dots, k\} = \{(c_i, t_i), i = 1, 2, \dots, k\}$, where c_i signifies the center of the granular ball, t_i is the label of GB_i and k is the number of generated granular balls.
 - 17: Find the hidden layer features using (4).
 - 18: Create the enhanced features using (5).
 - 19: Compute w_1, b_1, w_2 , and b_2 using (18) and (19).
 - 20: Classify testing samples into class +1 or -1 using (22).
-

EF-GBT SVM to efficiently handle large datasets and demonstrate scalability. However, the TSVM's imperative demand for matrix inversions presents formidable obstacles to its efficiency and applicability on large-scale datasets.

- TSVM struggles to handle noise and outliers in datasets, whereas the proposed model addresses these challenges effectively by incorporating granular balls to generate optimal classifiers.

S.III Sensitivity Analyses

To comprehensively understand the robustness of the proposed models, it is essential to analyze their sensitivity to hyperparameters. Therefore, we conduct the following sensitivity analyses to delve deeper into the behavior of the models:

S.III.A Sensitivity Analysis of Hyperparameters d_1 and d_2

To thoroughly grasp the nuanced effects of hyperparameters on the model's generalization capability, we systematically explore the hyperparameter space by

varying the values of d_1 and d_2 . This exploration allows us to identify configurations that maximize predictive accuracy and enhance the model’s robustness to unseen data. The graphical representations in Fig S.1 offer visual insights into how parameter tuning affects the accuracy (ACC) of our EF-GBTSVM model in the linear case. These visuals illustrate significant variations in model accuracy across different d_1 and d_2 values, underscoring the sensitivity of our model’s performance to these hyperparameters. From Figs. S.1a and S.1b, the optimal performance of the proposed EF-GBTSVM model is observed within the d_1 and d_2 ranges of 10^{-1} to 10^5 and 10^{-3} to 10^5 , respectively. From Figs. S.1c and S.1d, the ACC of the proposed EF-GBTSVM model archives the maximum when d_1 and d_2 ranges of 10^{-3} to 10^5 , respectively. Therefore, we recommend using d_1 and d_2 from the range 10^{-3} to 10^5 for efficient results, although fine-tuning may be necessary depending on the dataset’s characteristics for the proposed EF-GBTSVM model to achieve optimal generalization performance.

S.III.B Effect of Parameter “Act fun” on the Performance of the Proposed EF-GBTSVM model

The activation function significantly influences the performance of the EF-GBTSVM model. In our experiment, we tuned nine different activation functions. The indexing of these functions is as follows: 1) SELU, 2) ReLU, 3) Sigmoid, 4) Sine, 5) Hardlim, 6) Tribas, 7) Radbas, 8) Sign, and 9) Leaky ReLU. We investigate the relationship using Fig S.2 across datasets including breast_cancer, chess_krvkp, haber, and heart-stat. Our observation highlights a sensitivity to “Act fun”. For instance, in the breast_cancer dataset, activation function 9 shows lower performance. Conversely, in the haber dataset, activation function 4 exhibits superior performance. This variability underscores the mixed performance across different datasets with respect to Act fun, suggesting the importance of fine-tuning the activation function to optimize results effectively.

S.III.C Influence of the numbers of hidden modes h

The impact of hyperparameter h (numbers of hidden nodes) is illustrated in Fig S.3. Our analysis reveals distinct trends for the EF-GBTSVM model. For thyroid dataset, the performance shows steady improvement with increasing h , plateauing at higher values like $h = 143$ or greater. Conversely, EF-GBTSVM for checkerboard_Data achieves peak performance at $h = 103$ and exhibits a gradual decline as h increases beyond this point. In conclusion, our results underscore the impact of dataset characteristics on the performance of the proposed EF-GBTSVM model, stressing the importance of fine-tuning the parameter h for optimal performance of the proposed EF-GBTSVM model.

S.IV Ablation Study

We conducted an ablation study on the EF-GBTSVM model to confirm the importance of granular balls in improving model performance. In this study, we

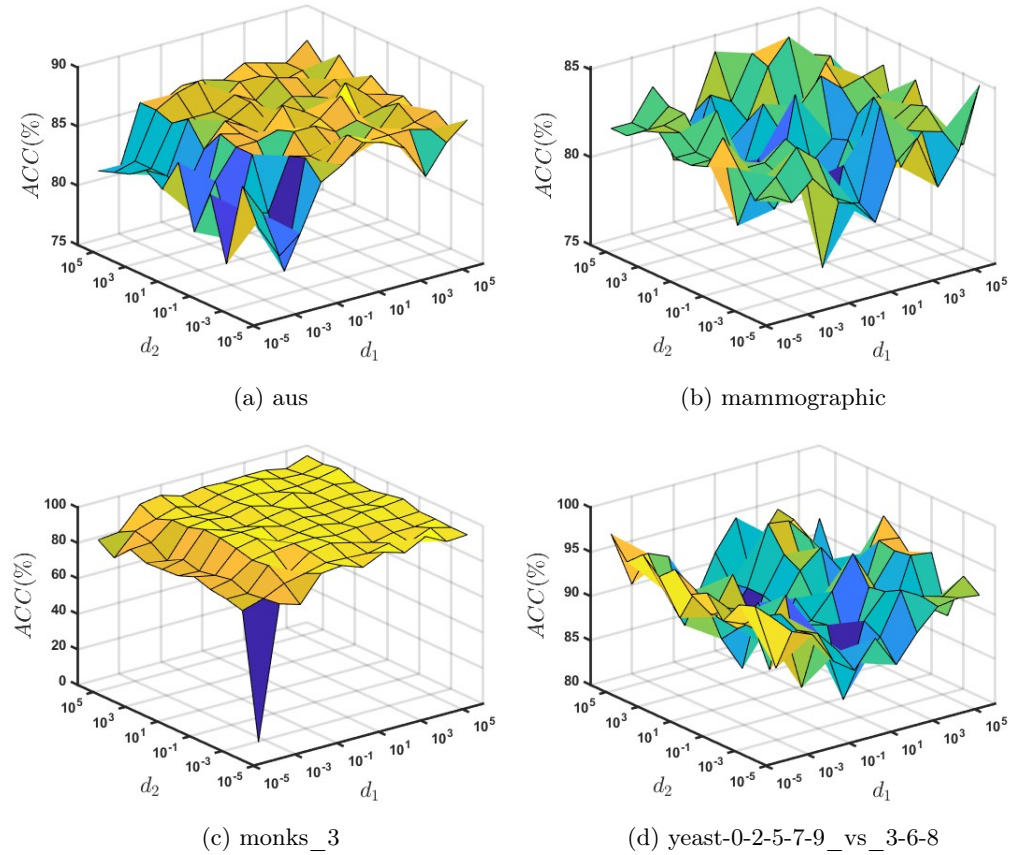


Fig. S.1: The effect of hyperparameter (d_1, d_2) tuning on the accuracy (ACC) of some UCI and KEEL datasets on the performance of EF-GBTSVM.

Dataset	TSVM [15]	RVFLwoDL [13]	RVFL [23]	HF-TSVM	HF-GBTSVM [†]	EF-TSVM	EF-GBTSVM [†]
aus	64.31	87.98	86.94	83.75	85.1	87.02	88.96
checkerboard_Data	64.31	85.98	85.94	43.75	85.1	87.02	86.21
chess_krvkp	67.41	90.2	90.41	69.04	90.09	97.5	98.16
haber	57.96	76.09	78.26	73	76.09	76.09	79.35
monks_3	59.7	43.11	43.11	82.608	88.62	93.41	92.22
Average ACC	62.74	76.67	76.93	70.43	85	88.21	88.98

[†] represents the proposed models.

Table S.1: Ablation study of the granular ball in the proposed EF-GBTSVM model compared with baseline TSVM, RVFLwoDL, and RVFL models over UCI and KEEL datasets.

compared the EF-GBTSVM model's performance against baseline models, including TSVM, RVFLwoDL, and RVFL. Additionally, we trained HF-GBTSVM and EF-GBTSVM models using the original input samples instead of the gen-

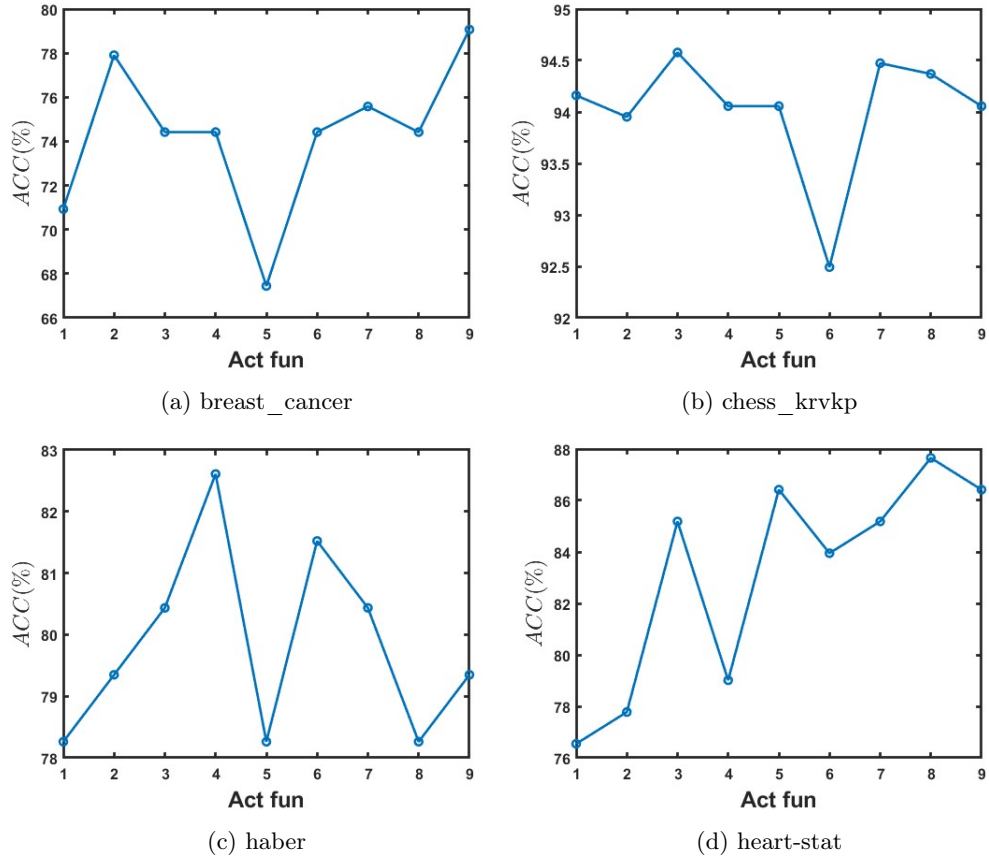
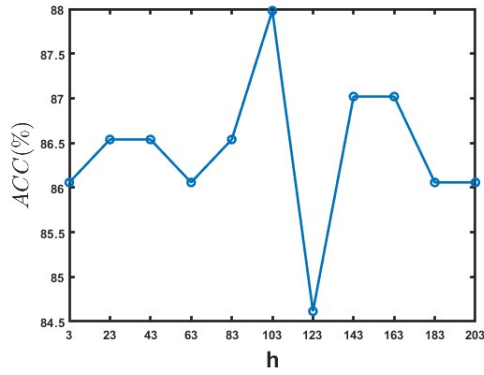


Fig. S.2: Effect of parameter “Act fun” on the performance of the proposed EF-GBTSVM model.

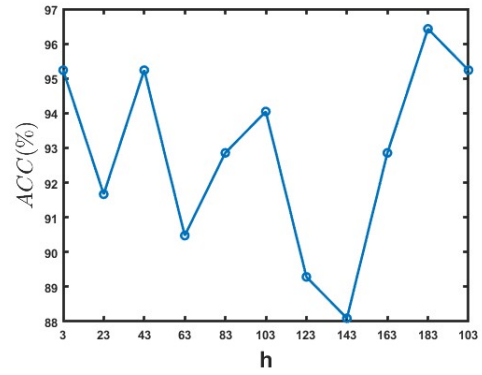
erated granular ball centers, referring to these as HF-TSVM and EF-TSVM models, respectively.

From the results shown in Table S.1, the EF-GBTSVM model demonstrated superior performance across most datasets, achieving an average accuracy (ACC) of 88.98%, the highest among the models compared. The EF-TSVM model followed closely with an average ACC of 88.21%. This indicates that using granular balls, along with extracting features in the enhanced feature space, is crucial for enhancing model performance.

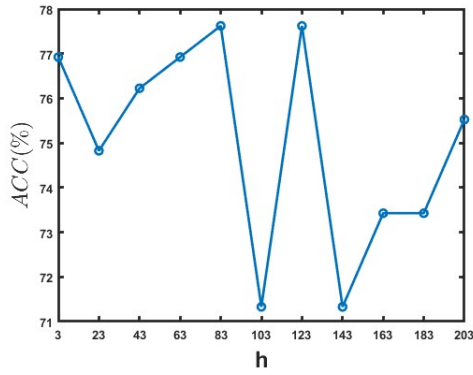
The ablation study highlights the significance of granular balls in the EF-GBTSVM model. By comparing the models trained with and without granular ball centers, we observed a clear performance advantage when incorporating granular balls. This suggests that the granular ball approach not only helps in capturing the underlying data structure but also improves the robustness and ACC of the



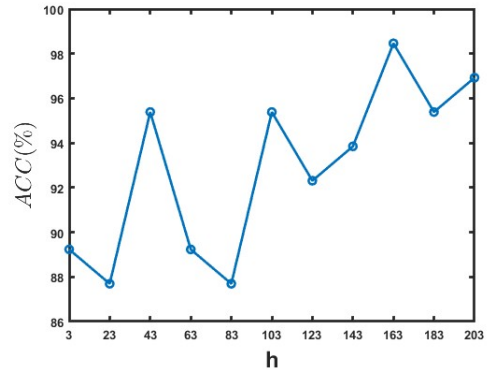
(a) checkerboard_Data



(b) ecoli-0-1-4-6_vs_5



(c) musk_1



(d) thyroid1

Fig. S.3: Effect of parameter h on the performance of the proposed EF-GBT SVM model.

model. The study underscores the critical role of both the granular ball framework and feature extraction in the enhanced feature space in achieving superior classification results.